Approximate-master-equation approach for the Kinouchi-Copelli neural model on networks

Chong-Yang Wang,[1] Zhi-Xi Wu,[1,*] and Michael Z. Q. Chen[2,†]

[1]*Institute of Computational Physics and Complex Systems, Lanzhou University, Lanzhou, Gansu 730000, China*

[2]*Department of Mechanical Engineering, The University of Hong Kong, Pokfulam Road, Hong Kong, P. R. China*

(Received 22 August 2016; revised manuscript received 12 October 2016; published 12 January 2017)

In this work, we use the approximate-master-equation approach to study the dynamics of the Kinouchi-Copelli neural model on various networks. By categorizing each neuron in terms of its state and also the states of its neighbors, we are able to uncover how the coupled system evolves with respective to time by directly solving a set of ordinary differential equations. In particular, we can easily calculate the statistical properties of the time evolution of the network instantaneous response, the network response curve, the dynamic range, and the critical point in the framework of the approximate-master-equation approach. The possible usage of the proposed theoretical approach to other spreading phenomena is briefly discussed.

DOI: 10.1103/PhysRevE.95.012310

I. INTRODUCTION

Most experimental studies in psychophysics have focused on the relationship between physical stimuli and the psychological feelings produced by them [1,2]. In general, the physical stimuli can be in the form of light, sound, pressure, and so on, and the psychological feelings can be the responses of vision, hearing, touch, etc. Experimentally, two classical results in psychophysics have been put forward, namely the logarithm function $F(r) \sim \log r$ (the Weber-Fechner law) and the power-law function $F(r) \sim r^h$ (the Stevens law), where $F(r)$ describes the intensity of the psychological feelings, r is the intensity of the physical stimuli, and h is the fitting exponent [1,2]. Up to now, a large number of theoretical models have been proposed to explain these experimentally observed psychophysical laws [3,4], and these models have made significant contributions toward explaining how the brain works [5,6], how neurons transmit signals [7], and many other interesting phenomena in neural science.

With the crucial experimental finding that the electrical coupling by gap junctions is immanent in many sensory systems (e.g., the olfactory glomeruli [8,9] and the retina [10]), Kinouchi and Copelli proposed a neural model on the Erdös-Rényi (ER) random networks to characterize the neural activity connected by electrical synapses [3]. It was found that the sensitivity (the extent of the response of the system to small physical stimuli) and the dynamic range (the number of decades over which the physical stimulus can be properly discriminated [3]) are maximized at a special value (the critical point [3]) of the coupling parameter among neurons. Moreover, the same phenomenon has also been observed when the model is built on a scale-free network [11,12]. In Refs. [13,14], Larremore *et al.* developed a general theoretical approach to study the dynamic range of the Kinouchi-Copelli neural model on networks. They found that the dynamic range is closely determined by the topology (say, the largest eigenvalue of the adjacency matrix) of the underlying interaction networks. Pei *et al.* [15] found that introducing an inhibitory factor for each excitatory node can enhance the network dynamic range.

So far, the Kinouchi-Copelli neural model has been used to explain a series of interesting phenomena that were found experimentally in neural systems or general excitable systems, such as nonlinear response functions in sensory systems [1], maximum dynamic range at criticality in the cortical networks [16], the scaling properties expected at criticality in brain dynamics [17], etc. Most existing studies are mainly based on either Monte Carlo simulations [3,18] or general mean-field approximate analysis [12,19,20]. As is well known, for self-organized critical systems, the results from stochastic simulations in the vicinity of criticality inevitably display great fluctuations caused by many factors, such as the randomness of the construction of networks and the intrinsic randomness in the dynamical process (including the probabilistic dynamics of the external stimulus and the influence from neighbors). To obtain the critical point more precisely, one has to increase the network size substantially and carry out extensive simulations, which is very computationally cost.

In this paper, we study the statistical properties of the Kinouchi-Copelli neural model on diverse networks by using the approximate-master-equation approach (AMEA), with which the dynamical states of the system are characterized by a set of ordinary differential equations. Once the initial conditions are given, we can trace the evolution of the system deterministically. As will be shown below, the results from the AMEA and the stochastic simulations are in excellent agreement, such as the time evolution of the network instantaneous response (the density of excited neurons at a given time), the network response curve (the density of excited neurons averaged over a large time window), and the dynamic range. Remarkably, with the AMEA, we are able to find the critical point more accurately and efficiently, yet in an easier manner in comparison to direct stochastic simulations.

II. THE KINOUCHI-COPELLI NEURAL MODEL

The Kinouchi-Copelli neural model is a simple excitable model for neural activity consisting of N coupled excitable neurons [3]. The instantaneous membrane potential of the ith neuron at time t is represented by $s_i(t) \in \{0,1,\ldots,n-1\}$, where $n \geqslant 3$. The state $s_i(t) = 0$ denotes the resting state, $s_i(t) = 1$ represents the excited state, and the remaining $s_i(t) = 2,\ldots,n-1$ account for the refractory period. When

*wuzhx@lzu.edu.cn

†mzqchen@outlook.com

the ith neuron is in the resting state at time t, there are two ways for it to transfer to the excited state at time $t+1$: (a) From the external stimulus, modeled by a Poisson process with rate r (which implies a transition with probability $\lambda = 1-\exp(-r\Delta t)$ per time step, and we assume $\Delta t = 1$ ms as in [3]); (b) from the influence (with probability p) of each currently excited neighbor j. p is also referred to as the branching probability in the branching processes [21], where the branching ratio $\sigma = Kp$ describes the expected number of excited neurons stimulated by an excited neuron in the next time step. For neurons with $s_i(t) \geqslant 1$, the dynamics is deterministic: $s_i(t+1) = [s_i(t)+1] \bmod n$, regardless of the external stimulus or the influence coming from the excited neighbors. After the neuron is excited, the refractory period takes place subsequently, during which time the neuron cannot be excited until it returns to a resting state again.

III. APPROXIMATE-MASTER-EQUATION APPROACH

The AMEA has been widely used in solving the epidemic spreading problem [22,23] and in the binary-state dynamics on networks [24,25]. Here, we attempt to apply the AMEA to the Kinouchi-Copelli neural model. For simplicity, we will consider herein only three possible states of each neuron: resting, excited, and refractory (i.e., we set $n = 3$, and the theoretical treatment can be straightforwardly extended to the case of $n > 3$). Each neuron can then be categorized by its state, say, the resting state (R), the (excited) spiking state (S), the refractory state (T), and by the number of its neighbors in each state. Let $R_{i,j,l}$ be the number of resting neurons with i resting neighbors, j excited neighbors, and l refractory neighbors. $S_{i,j,l}$ and $T_{i,j,l}$ can be defined in a similar way (note that these neurons have a total degree $i+j+l$). Since a neuron in the resting state can be excited by an external stimulus with probability λ, or by each excited neighbor with probability p, independently, then a neuron belonging to the $R_{i,j,l}$ class will be excited with probability $[1-(1-p)^j(1-\lambda)]$. Note that $(1-p)^j(1-\lambda)$ characterizes the expected probability that a neuron belonging to the $R_{i,j,l}$ class will not be stimulated to exciting by the influences from both those excited neighbors and the external stimulus. Then, the total number of new excited neurons at one time step is $\sum_{k=0}^{k_{\max}}\sum_{i+j+l=k} R_{i,j,l}[1-(1-p)^j(1-\lambda)]$. These new excited neurons cause their resting neighbors to change their *effective* degree (available for influence) at the rate $\sum_{k=0}^{k_{\max}}\sum_{i+j+l=k} iR_{i,j,l}[1-(1-p)^j(1-\lambda)]$. With the total number of the resting neighbors of R neurons $\sum_{k=0}^{k_{\max}}\sum_{i+j+l=k} iR_{i,j,l}$, we yield the probability that one resting neighbor of the R neurons is going to be excited as

$$P_R = \frac{\sum_{k=0}^{k_{\max}}\sum_{i+j+l=k} iR_{i,j,l}[1-(1-p)^j(1-\lambda)]}{\sum_{k=0}^{k_{\max}}\sum_{i+j+l=k} iR_{i,j,l}}. \quad (1)$$

Similarly, the probability that one resting neighbor of the S neurons is going to be excited is

$$P_S = \frac{\sum_{k=0}^{k_{\max}}\sum_{i+j+l=k} jR_{i,j,l}[1-(1-p)^j(1-\lambda)]}{\sum_{k=0}^{k_{\max}}\sum_{i+j+l=k} iS_{i,j,l}}, \quad (2)$$

and the probability that one resting neighbor of the T neurons is going to be excited is

$$P_T = \frac{\sum_{k=0}^{k_{\max}}\sum_{i+j+l=k} lR_{i,j,l}[1-(1-p)^j(1-\lambda)]}{\sum_{k=0}^{k_{\max}}\sum_{i+j+l=k} iT_{i,j,l}}. \quad (3)$$

The schematic illustration of the AMEA for the Kinouchi-Copelli neural model is shown in Fig. 1. For convenience, we denote the number of neurons in each state at time t by $X_{i,j,l}(t)$, where $X \in \{R,S,T\}$. The time variation of $X_{i,j,l}(t)$ will be due to either the change of the states of the neurons themselves, or the change of the states of their neighbors (altering the subscripts). First, we consider the state transformation of

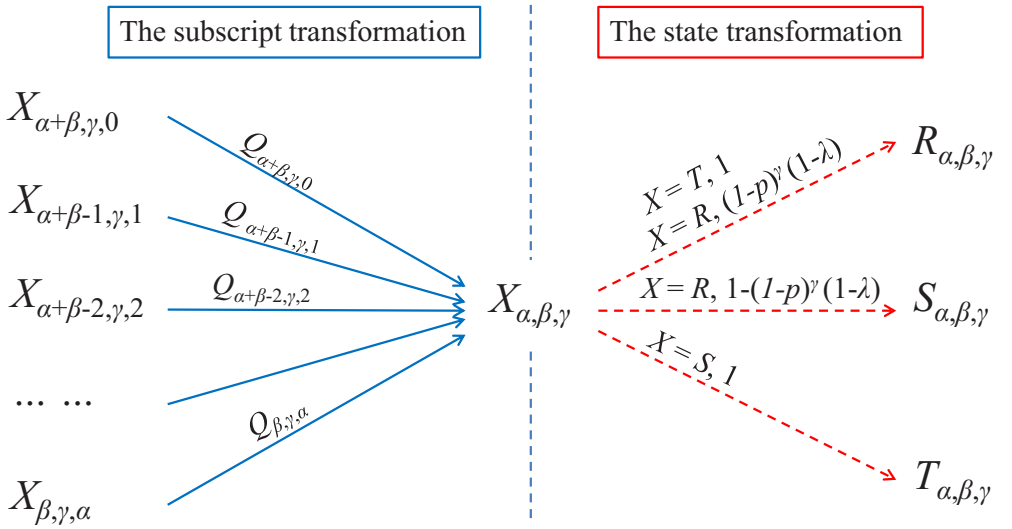

FIG. 1. Schematic illustration of the approximate-master-equation approach for the Kinouchi-Copelli neural model. The solid arrows represent the changes in the states of the neurons' neighbors (subscript transformation), and the dashed arrows represent the changes in the state of the focal neuron X itself ($X \in \{R,S,T\}$, state transformation). $X_{\alpha,\beta,\gamma}$ is an intermediate state, the expressions $Q_{\alpha+\beta-l,\gamma,l}$ ($Q \in \{G,H,O\}$, $l \in \{0,1,2,\ldots,\alpha\}$) denote the probabilities of the subscript transformation, and the expressions above the dashed arrows indicate the probabilities of the change of different X. See more details in the corresponding text.

the neighbors of the neurons, i.e., how $X_{i,j,l}(t)$ changes to $X_{\alpha,\beta,\gamma}(t+1)$, which we call the subscript transformation, as shown in the left part of Fig. 1. Obviously, the subscripts satisfy the relationship $i+j+l=\alpha+\beta+\gamma$. Moreover, since the states of the neurons change deterministically after being excited, the j excited neighbors will go into the refractory period, the l refractory neighbors will go directly into the resting state, and we have $\gamma=j$. Thus, if a neuron is in the $X_{\alpha+\beta-l,\gamma,l}(t)$ class at time t and its β resting neighbors are going to be excited, then it will join the $X_{\alpha,\beta,\gamma}(t+1)$ class at time $t+1$. Consequently, the probability of the subscript transformation for $R_{\alpha+\beta-l,\gamma,l}$ can be expressed as

$$G_{\alpha+\beta-l,\gamma,l}=\binom{\alpha+\beta-l}{\beta}P_R^{\beta}(1-P_R)^{\alpha-l}, \tag{4}$$

where the prefactor is the binomial coefficient. Similarly, the probability of the subscript transformation for $S_{\alpha+\beta-l,\gamma,l}$ can be obtained as

$$H_{\alpha+\beta-l,\gamma,l}=\binom{\alpha+\beta-l}{\beta}P_S^{\beta}(1-P_S)^{\alpha-l}, \tag{5}$$

and the probability of the subscript transformation for $T_{\alpha+\beta-l,\gamma,l}$ can be obtained as

$$O_{\alpha+\beta-l,\gamma,l}=\binom{\alpha+\beta-l}{\beta}P_T^{\beta}(1-P_T)^{\alpha-l}. \tag{6}$$

Besides the subscript transformation, we need to consider the state transition of the neurons themselves, which we call the state transformation, as shown in the right part of Fig. 1. The probability that a neuron in the $R_{\alpha,\beta,\gamma}(t)$ class still remains in the same class at the next time step is $(1-p)^{\beta}(1-\lambda)$, which means that it is not excited by either the external stimulus or the influence from those excited neighbors. The probability that a neuron in the $R_{\alpha,\beta,\gamma}(t)$ class joins the $S_{\alpha,\beta,\gamma}(t+1)$ class at the next time step is $[1-(1-p)^{\beta}(1-\lambda)]$. Due to the deterministic state transformation of the excited and refractory neurons, the probability that a neuron in the $S_{\alpha,\beta,\gamma}(t)$ class joins the $T_{\alpha,\beta,\gamma}(t+1)$ class, and that a neuron in the $T_{\alpha,\beta,\gamma}(t)$ class joins the $R_{\alpha,\beta,\gamma}(t+1)$ class, are both equal to 1.

Now, in the framework of the AMEA, the dynamics of the Kinouchi-Copelli neural model on a static uncorrelated network can be described by the following $(k_{\max}+1)(k_{\max}+2)(k_{\max}+3)/6$ equations:

$$\begin{aligned}
R_{\alpha,\beta,\gamma}(t+1)&=\sum_{l=0}^{\alpha}\{R_{\alpha+\beta-l,\gamma,l}(t)G_{\alpha+\beta-l,\gamma,l}[(1-p)^{\gamma}(1-\lambda)]\\
&\quad+T_{\alpha+\beta-l,\gamma,l}(t)O_{\alpha+\beta-l,\gamma,l}\},\\
S_{\alpha,\beta,\gamma}(t+1)&=\sum_{l=0}^{\alpha}\{R_{\alpha+\beta-l,\gamma,l}(t)G_{\alpha+\beta-l,\gamma,l}\\
&\quad\times[1-(1-p)^{\gamma}(1-\lambda)]\},\\
T_{\alpha,\beta,\gamma}(t+1)&=\sum_{l=0}^{\alpha}\{S_{\alpha+\beta-l,\gamma,l}(t)H_{\alpha+\beta-l,\gamma,l}\},
\end{aligned} \tag{7}$$

where $\alpha+\beta+\gamma=k$, and $k\in\{0,1,\ldots,k_{\max}\}$ is the degree of the neurons in the network.

Initially, we randomly choose a fraction ρ_0 (we set $\rho_0=0.1$) of neurons in the network as excited seeds so that the initial condition can be written as

$$\begin{aligned}
R_{\alpha,\beta,\gamma}(0)&=\begin{cases}N(1-\rho_0)B_{\alpha+\beta+\gamma,\beta}(\rho_0)P_k, & \gamma=0,\\ 0, & \gamma\neq 0,\end{cases}\\
S_{\alpha,\beta,\gamma}(0)&=\begin{cases}N\rho_0 B_{\alpha+\beta+\gamma,\beta}(\rho_0)P_k, & \gamma=0,\\ 0, & \gamma\neq 0,\end{cases}\\
T_{\alpha,\beta,\gamma}(0)&=0,
\end{aligned} \tag{8}$$

where P_k is the probability that a randomly chosen neuron has k neighbors, and $B_{\alpha+\beta+\gamma,\beta}(\rho_0)$ is the binomial factor,

$$B_{\alpha+\beta+\gamma,\beta}(\rho_0)=\binom{\alpha+\beta+\gamma}{\beta}\rho_0^{\beta}(1-\rho_0)^{\alpha}. \tag{9}$$

With the initial conditions Eq. (8), we can trail the values of different $X_{\alpha,\beta,\gamma}$ by iterating Eq. (7) directly, and we obtain deterministic results for the system in the long-time limit.

IV. STOCHASTIC SIMULATIONS AND ANALYSIS

A. Construction of the underlying interaction networks

We consider the Kinouchi-Copelli neural model on three types of uncorrelated networks: the Erdös-Rényi (ER) random network [26], a random regular graph (RRG) [27], and an uncorrelated random scale-free (SF) network [28,29]. In particular, we generate the ER random network by assigning each of the $NK/2$ links to a repeatedly and randomly chosen pair of nodes, which produces a random network with an average degree K and with a Poisson degree distribution $P_k=e^{-K}\frac{K^k}{k!}$. The RRG is also called the K-regular random graph or the Bethe lattice, with all nodes having the same degree K (i.e., $P_k=\delta_{k,K}$), which can be constructed by assigning each node K stubs exactly, and then pairing two randomly selected stubs consecutively, until all the stubs have been used up. Finally, we use the configuration algorithm to generate uncorrelated random SF networks [28,29]. Multiple connections and self-connections are forbidden in all cases.

B. Results and analysis

To specify the neural activity, we adopt the network response F, which is defined as in Ref. [3],

$$F=\frac{1}{\mathcal{T}}\sum_{t=1}^{\mathcal{T}}\rho_t, \tag{10}$$

where $\mathcal{T}$ is a large time window and ρ_t is the network instantaneous response (which is defined as the density of excited neurons at a given time t). Hence, F represents the mean exciting rate for the initial transduction from a physical stimulus to neural activity of the neural network. We calculate the dynamic range Δ of the response curve for a given branching probability p as [3]

$$\Delta=10\log\frac{r_{0.9}}{r_{0.1}}, \tag{11}$$

where $r_{0.1}$ and $r_{0.9}$ are the stimulus intensities corresponding to $F_{0.1}$ and $F_{0.9}$, respectively. Here, $F_x=F_0+x(F_{\max}-F_0)$, where F_0 ($F_{\max}$) is the minimum (maximum) network response [3]. Note that the minimum network response F_0 is always 0 for the subcritical and critical cases, since

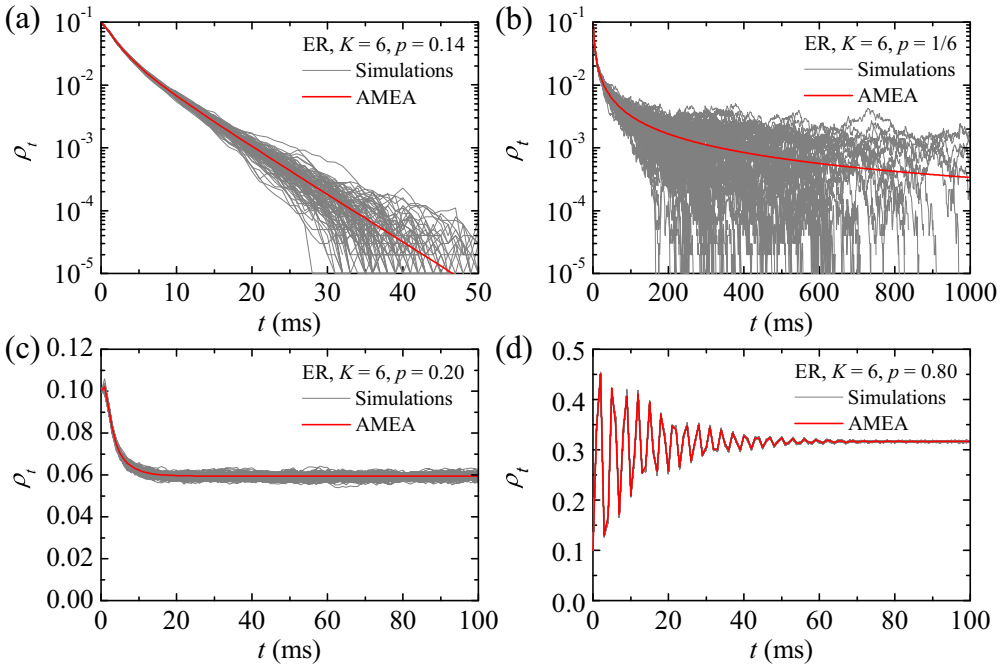

FIG. 2. Time series of the network instantaneous response ρ_t on the ER random networks with $K = 6$ and without an external stimulus (i.e., $r = 0$). (a) In the subcritical regime with $p = 0.14$, (b) at the critical point with $p = 1/6$, (c) in the supercritical regime with $p = 0.2$, and (d) in the supercritical regime with $p = 0.8$. Results from the AMEA are depicted by the thick solid lines (for just one realization), and those from stochastic simulations are represented by the thin solid lines (for 100 independent realizations).

neural activity vanishes in the long-time limit ($\rho_t = 0$), while it remains as a finite positive value in the supercritical region.

Let us first present in Fig. 2 the results of the Kinouchi-Copelli neural model on the ER random networks without external stimulus (i.e., $r = 0$). The instantaneous response from stochastic simulations is in the form of 100 independent realizations with parameters $N = 10^5$, $n = 3$, $K = 6$, and $\rho_0 = 0.1$. The time evolution of the network instantaneous response ρ_t calculated by the AMEA in terms of Eq. (7) is in good agreement with the results from stochastic simulations. The properties of our results are qualitatively similar to those in Ref. [3]. In the subcritical region ($p < p_c$), the activity stops in a very short period of time [see Fig. 2(a)] because the branching probability p between the resting neurons and the excited ones is not large enough to excite the resting ones, and the network instantaneous response ρ_t decays to zero in an exponential form [see Fig. 3(a)]. For the critical case ($p = p_c$), previous work showed that the activity has a large interval of extinction times [3]; see Fig. 2(b). Results from the AMEA show that the network instantaneous response ρ_t decays to zero in a power-law form [the thick solid lines obtained by the least-squares fitting method in Fig. 3(a)]. This property is very useful in finding the location of the critical point accurately. In the supercritical region ($p > p_c$), the system maintains self-sustained oscillations even in the absence of external stimulus [see Fig. 2(c)]. The activity in the supercritical region with large branching probability p needs to go through a long period of oscillations before reaching the stable state [see Fig. 2(d)].

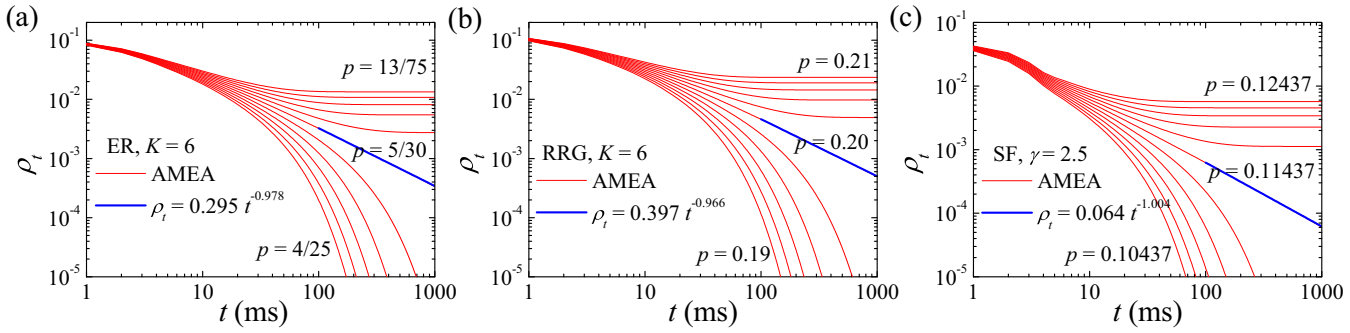

FIG. 3. The network instantaneous response ρ_t as a function of time t on (a) the ER random network with $K = 6$, (b) the RRG with $K = 6$, and (c) the uncorrelated random SF network with $\gamma = 2.5$ and without external stimulus ($r = 0$). Results from the AMEA are given by the thin solid lines, and the least-squares estimation of the closest power-law form for the critical state with $100 \leqslant t \leqslant 1000$ ms is displayed by thick solid lines.

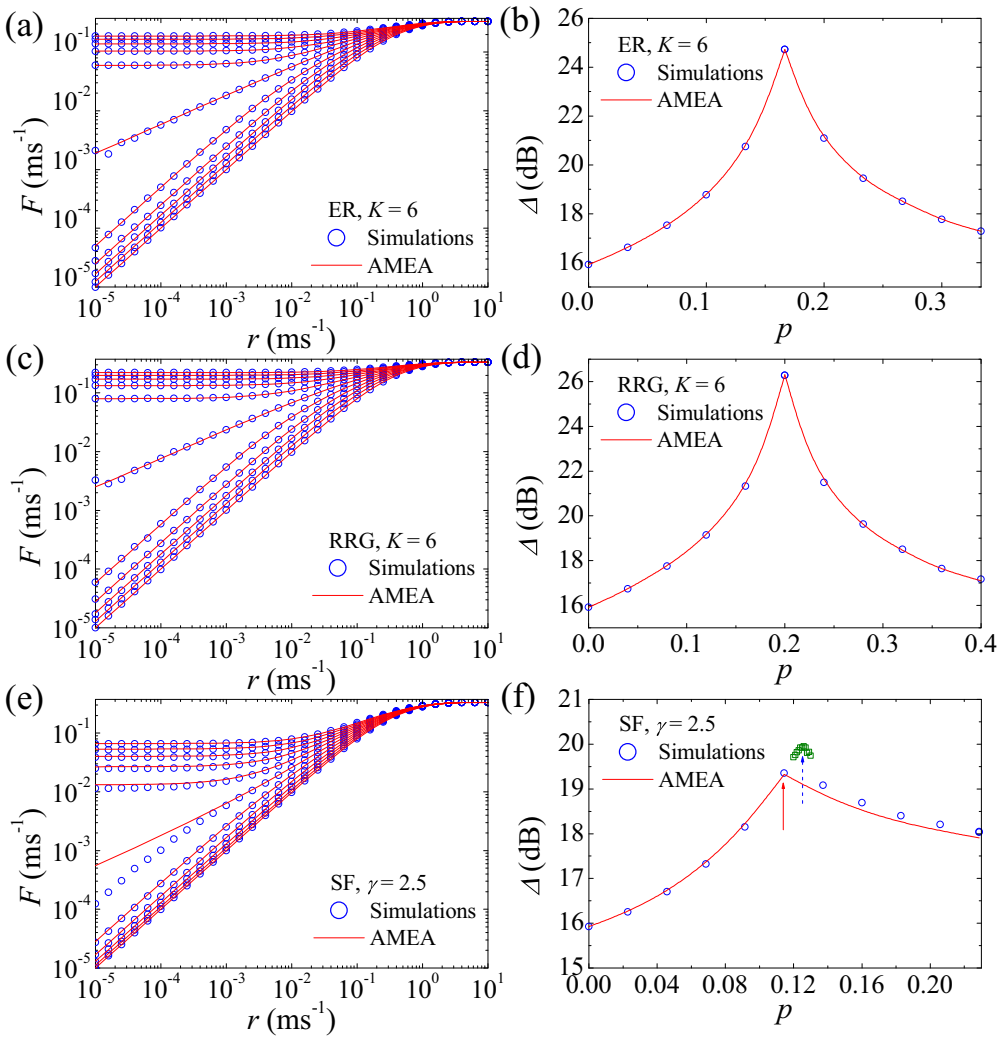

FIG. 4. Response curves F of the Kinouchi-Copelli neural model on (a) ER random networks with $K = 6$ (from $p = 0$ to 1/3 in intervals of 1/30), (c) RRGs with $K = 6$ (from $p = 0$ to 0.4 in intervals of 0.04), and (e) uncorrelated random SF networks with $\gamma = 2.5$ (from $p = 0$ to 0.228 74 in intervals of 0.022 874). Results from stochastic simulations on uncorrelated random SF networks are averaged over 100 independent realizations. Dynamic range Δ vs the branching probability p on (b) ER random networks with $K = 6$, (d) RRGs with $K = 6$, and (f) uncorrelated random SF networks with $\gamma = 2.5$. The olive squares in (f) represent the results for $p = 0.12$–0.13 (in intervals of 0.001) with the additional stochastic simulations. The dashed and solid arrows represent the critical points obtained by stochastic simulations and the AMEA, respectively.

As can be seen from Figs. 2 and 3, the results from stochastic simulations display noticeable fluctuations, especially in the region of criticality, while those from the AMEA are smooth curves without fluctuations (we have checked that the averaged results from a great number of realizations of stochastic simulations do converge to the estimations by the AMEA for the same given parameters, which are not shown here). As such, we can see that it is easier and more convenient for us to study the dynamical behavior (e.g., characterizing the neural activity, finding the critical point) of the Kinouchi-Copelli neural model on static uncorrelated networks by means of the AMEA.

Next, we focus on the dependence of the network response $F(r)$ on the branching probability p. Here, we would like to point out that one should measure the network response $F(r)$ over a sufficiently long time, otherwise the interval of the network instantaneous response (before reaching its steady state) will affect the results considerably. Figure 4 displays the response curves $F(r)$ and the dynamic range Δ of the Kinouchi-Copelli neural model on the ER random networks, RRGs, and uncorrelated random SF networks. Results from the AMEA (solid lines) and stochastic simulations (circles) coincide well with each other on the ER random networks [Figs. 4(a) and 4(b)] and the RRGs [Figs. 4(c) and 4(d)], while there arise slight discrepancies on the uncorrelated random SF networks. As shown in Figs. 4(e) and 4(f), the response curves $F(r)$ and the dynamic range Δ from both approaches are almost the same in the subcritical regime, but deviations arise in the critical regime and the supercritical regime. The dashed and the solid arrows in Fig. 4(f) indicate the critical points obtained from the stochastic simulations $p_c^{\mathrm{STO}} \approx 0.124$ and the AMEA $p_c^{\mathrm{AMEA}} \approx 0.114\,37$, respectively. We note that $p_c^{\mathrm{STO}} \geqslant p_c^{\mathrm{AMEA}}$. [The critical point, yielded by the reciprocal of the largest eigenvalue of the adjacency matrix of the underlying

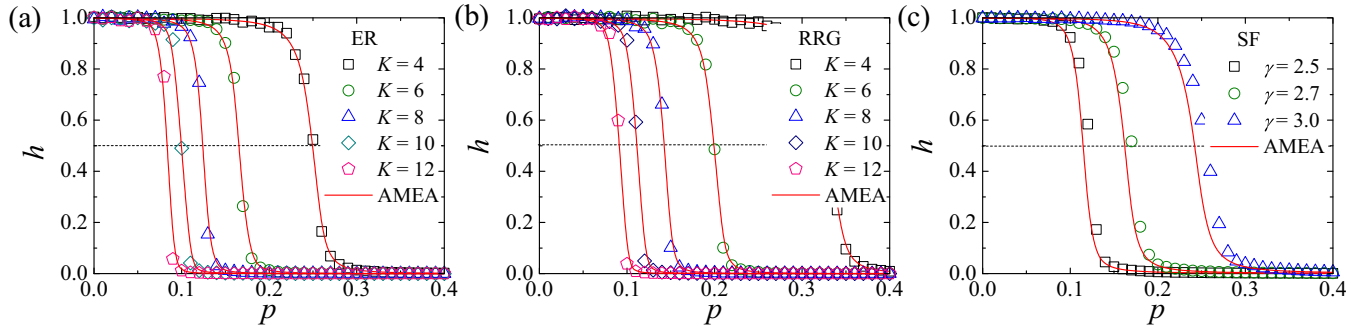

FIG. 5. The exponent h, which is obtained by doing the least-squares fitting of the response curves F with $10^{-5} \leqslant r \leqslant 10^{-3}$ ms^{-1} according to the relationship $F \sim r^h$, as a function of the branching probability p on (a) ER random networks, (b) RRGs, and (c) uncorrelated random SF networks. Parameters are the same as those in Fig. 4. Clearly, the exponent h is close to 1 for the uncoupled networks ($p = 0$), close to 1/2 at the critical point ($p = p_c$), and decreases to 0 in the supercritical regime ($p = 1$).

SF interaction networks in Fig. 4(f), is approximately equal to 0.087 881 [13,14], which suggests that the critical point obtained by the AMEA is more accurate.] Accordingly, the maximum dynamic range $\Delta_{\max}^{\mathrm{STO}}$ in the critical point obtained by stochastic simulations is greater than $\Delta_{\max}^{\mathrm{AMEA}}$ predicted by the AMEA. We have checked that the deviations will decrease with the increase of the network size N (not shown here).

It was demonstrated that the network response in the uncoupled case ($p = 0$) is given by $F = \lambda/[1 + (n-1)\lambda]$ and the maximum response scales with the refractory period as $F_{\max} = 1/n$ [3,11,12,30,31]. As shown in Fig. 4, our AMEA also gives correct theoretical estimations. Moreover, for sufficiently small external stimuli r, it was shown that the network response $F(r)$ changes linearly in the log-log scale, resulting in the relation $F \sim r^h$ (the Stevens law), where the exponent h changes from $h = 1$ in the subcritical regime (the uncoupled case with $p = 0$) to $h = 1/2$ at the critical point ($p = p_c$), and it decreases to 0 in the supercritical regime ($p = 1$) [3]. Once again, as shown in Fig. 5, our AMEA predicts the same dynamical behavior of $F(r)$. In addition, since the curves from the AMEA are usually smooth and continuous, it is also convenient for us to identify the critical point p_c by checking the position where $h = 1/2$ (see Fig. 5).

In the supercritical regime ($p > p_c$), the minimum response F_0 is not zero because of the self-sustained activity induced by the strong branching probability. Noticing that $F_0 = 0$ for the subcritical and critical cases. Then we can estimate the critical point by calculating the minimum response F_0 as a function of the branching probability p, and the results are summarized in Fig. 6. It is evident that the positions of the critical point for different networks are determined by the degree distribution and the average degree. In the next section, we give an approximate theoretical estimation for the critical position.

Up to now we have mainly studied the Kinouchi-Copelli model, in which all the neurons update their states synchronously. It is worth pointing out that the asynchronous updating neural network models have also played a huge role in pattern recognition, artificial intelligence, communication, control, finance, bioinformatics, and so on [32]. The simulation results and theoretical analysis of the Kinouchi-Copelli neural model with asynchronous update are summarized in Appendix C. We find that the results for both synchronous and asynchronous Kinouchi-Copelli models are qualitatively consistent.

V. THE CRITICAL POINT

Critical phenomena in complex networks are a popular research topic [33]. Previous research has suggested that the dynamical behavior at the critical point of a complex system is connected with optimal computational capabilities [34], optimal transmissions [35], and sensitivity to sensory stimuli [3,36,37]. Recently, experiments in neural networks showed that the dynamic range will be maximized and a power-law distribution of neuronal avalanches emerges at

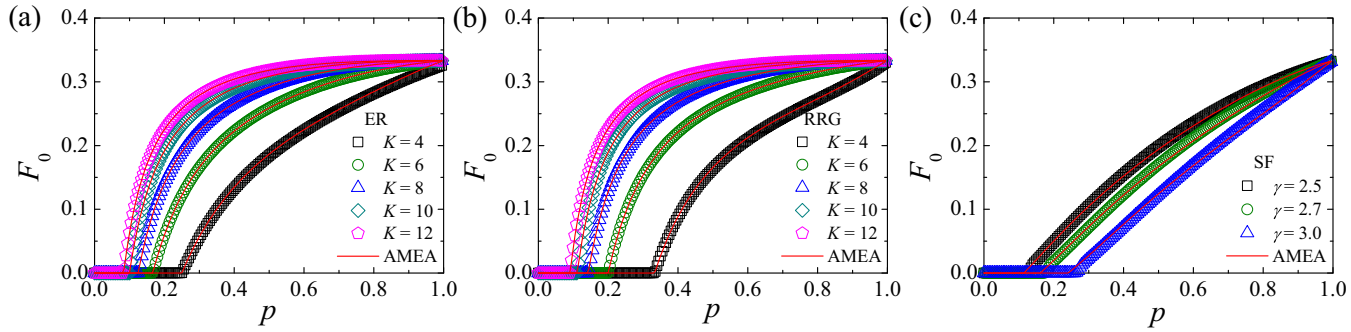

FIG. 6. Minimum response F_0 as a function of the branching probability p of the Kinouchi-Copelli neural model on (a) ER random networks, (b) RRGs, and (c) uncorrelated random SF networks.

TABLE I. Estimated critical points by using the least-squares estimate of the closest power-law decay form ($\rho_t \sim t^{-h_t}$) for the network instantaneous response ρ_t with $100 \leqslant t \leqslant 1000$ ms on ER random networks, RRGs, and uncorrelated random SF networks. The results here are more accurate than those in Fig. 3.

ER			RRG			SF		
K	p_c	h_t	K	p_c	h_t	γ	p_c	h_t
4	0.24997	1.00000	4	0.33325	1.00140	2.5	0.11437	1.00424
6	0.16664	1.00228	6	0.19995	1.00406			
8	0.12498	1.00485	8	0.14282	1.00660	2.7	0.16151	1.00159
10	0.09998	1.00579	10	0.11109	0.99655			
12	0.08332	1.00006	12	0.9089	0.99991	3.0	0.24149	1.00043

the critical point [16,38], which is consistent with the earlier theoretical predictions [17,39–41]. An important question then is how the critical point can be found accurately before studying the critical behavior or the behavior near the critical point. In Appendix A, we apply the mean-field theory to the Kinouchi-Copelli neural model, and we find that its applicability is quite limited.

In Sec. IV, we have presented three methods to estimate the critical point, which are all based on the AMEA. (Note that the maximum of the power spectral density of neuronal activity fluctuations can give, in some cases, a better estimation of the critical point of both first- and second-order phase transitions in neuronal networks [42,43].) The first is the minimum response F_0 as a function of the branching probability p. The second is the power-law decay behavior of the network instantaneous response ρ_t. The third one corresponds to the power-law growth behavior (with exponent $h = 1/2$) of the response F as a function of r in the case of weak external stimulus ($\lesssim 10^{-3}$ ms^{-1}). Generally, we can obtain a fairly accurate critical point using a combination of these three methods. In Table I, we list the critical points obtained by doing the least-squares estimation of the closest power-law decay form for the network instantaneous response ρ_t ($100 \leqslant t \leqslant 1000$ ms) on the ER random networks, RRGs, and uncorrelated random SF networks. It is worth pointing out that the maximum likelihood method [44] will generally give a better estimation of the exponent than the least-squares method does. In Fig. 7, we plot the critical point p_c as a function of the average degree K for the cases of the ER random networks and RRGs, and we obtain two simple relations, $p_c^{\mathrm{ER}} \sim \frac{1}{K}$ and $p_c^{\mathrm{RRG}} \sim \frac{1}{K-1}$.

In the remainder of this section, we present approximate theoretical derivations for these expressions by using the AMEA. For simplicity, we consider the Kinouchi-Copelli neural model on RRGs. There will be no neurons in an excited state in the subcritical regime, and at the critical point there may be a small number of neurons excited at the beginning, but this number will evolve to zero eventually. Thus, near the critical point, it is reasonable for us to just consider that the values of the subscripts j,l are equal to either 0 or 1. That means that we just consider the classes of $X_{K,0,0}$, $X_{K-1,1,0}$, and $X_{K-1,0,1}$, where $X \in \{R,S,T\}$ (all the other classes can be omitted reasonably). Combining these approximations with Eqs. (1)–(7), we can obtain the following equations:

$$\begin{aligned} AR_{K,0,0} + BR_{K-1,1,0} &= 0, \\ CR_{K,0,0} + DR_{K-1,1,0} &= 0, \end{aligned} \tag{12}$$

where the coefficients A,B,C,D are functions of K and p (for more details, see Appendix B). To obtain nonzero solutions of Eq. (12), the determinant of the coefficient matrix should be zero, which will lead to the following equation:

$$ap^2 + bp + c = 0, \tag{13}$$

where

$$\begin{aligned} a &= (2K-3)z^{2K-4} + (K^2 - 6K + 6)z^{K-2} \\ &\quad - (K-2)(K-1), \\ b &= -(K-1)z^{K-2} + K(K-1), \quad c = -1. \end{aligned} \tag{14}$$

We summarize in Fig. 7 the thresholds of the Kinouchi-Copelli neural model on (a) ER random networks, and (b) RRGs, with different average degree K, which have been calculated from stochastic simulations, the AMEA, and also the solutions of Eq. (13). All approaches have produced results essentially in agreement with each other. The numerical solutions of Eq. (13) give approximately a fairly simple

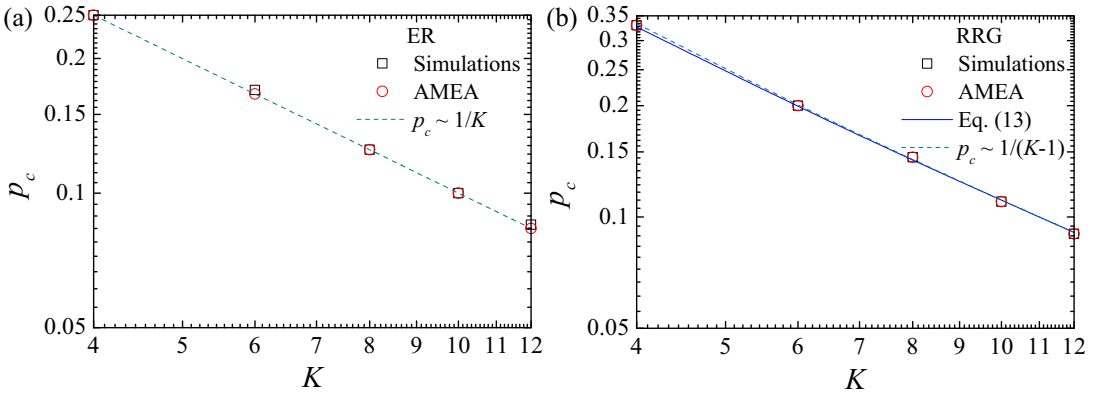

FIG. 7. The threshold p_c vs the average degree K on (a) ER random networks and (b) RRGs. The black squares are simulation results, the red circles are the results from the AMEA, the dashed lines are the linear fitting of the AMEA results in the log-log scale, and the solid line is the solution of Eq. (13). Other parameter values are the same as those in Fig. 6.

result,

$$p_c \approx \frac{1}{K-1}, \tag{15}$$

which is shown in Fig. 7(b).

VI. CONCLUSION

We have applied the approximate-master-equation approach to solve the Kinouchi-Copelli neural model on Erdös-Rényi random networks, random regular graphs, and uncorrelated random scale-free networks. Specifically, we perform comparative studies of the time evolution of the network instantaneous response, the network response curve, the dynamic range, and the minimum response by means of stochastic simulations as well as the AMEA. Results from both methods agree well with each other. A large number of investigations on neural activity have indicated that the dynamic range displays a maximum level at the critical point. The spontaneous activity that is optimized for input processing at criticality has also been found experimentally [16]. Critical behavior is an important characteristic for the study of neural activity. In the vicinity of the critical point, curves obtained from direct stochastic simulations usually display large fluctuations, which always hinder us in obtaining the accurate critical point of the Kinouchi-Copelli model at the first onset. To determine the critical point, we have to perform extensive computer simulations to smooth the curves, which is very computationally costly. We have demonstrated that the determination of the critical point via the AMEA is quite convenient and efficient. In particular, three different methods can be conveniently adopted to determine the location of the critical point in terms of the dynamical behavior of the network instantaneous response, the network response curve, and the dynamic range as a function of the time or the branching probability p.

Finally, we would like to point out that the AMEA can be easily generalized to more sophisticated neural models, such as the excitatory-inhibitory model [45] and the models with electrical and chemical synapses [46,47], which are more reasonable to model real neural networks. At the same time, this method should not be limited to the dynamics of the Kinouchi-Copelli neural model and epidemic spreading processes. It can also be applied to the analysis of opinion dynamics, information processing, and so on.

ACKNOWLEDGMENTS

We would like to thank J.-Q. Zhang, C.-R. Cai, and X.-S. Liu for fruitful discussions. This work was supported by the National Natural Science Foundation of China (Grants No. 61374053, No. 11475074, and No. 11575072).

APPENDIX A: MEAN-FIELD APPROACH

The Kinouchi-Copelli neural model can be analyzed by means of the mean-field theory [12,48]. For the cases of the RRGs and ER random networks, we assume that each neuron has the same number of neighbors $k \simeq K$, according to the homogeneous mixing hypothesis [48]. In the framework of the mean-field theory, the Kinouchi-Copelli neural model can be described as follows:

$$\partial_t \rho_t(1) = -\rho_t(1) + \lambda\rho_t(0) + (1-\lambda)\rho_t(0) \times [1-[1-p\rho_t(1)]^K], \tag{A1}$$

where $\rho_t(0)$ is the density of the resting neurons at time t. In the stationary state, we have $\rho_t(0) = 1-(n-1)\rho_t(1)$ [3,12,49]. The first term on the right-hand side in Eq. (A1) represents the excited neurons going into the refractory state with probability 1. The second term indicates the resting neurons becoming excited by the external stimulus with probability λ. The third term stands for the resting neurons becoming excited by the excited neighbors with probability p.

By imposing the stationarity condition $\partial_t \rho_t(1) = 0$, we obtain the equation

$$-\rho(1) + \lambda\rho(0) + (1-\lambda)\rho(0)[1-[1-p\rho(1)]^K] = 0. \tag{A2}$$

To view the critical behavior by the minimum response F_0 [without external stimulus ($\lambda = 0$)], we linearize the term $[1-p\rho(1)]^K$ in Eqs. (A2) around $p\rho(1) \to 0$, and we obtain

$$\rho(1) \approx \frac{1}{n-1}\left(1-\frac{1}{pK}\right), \tag{A3}$$

which is reasonable when p or $\rho(1)$ is sufficiently small. Therefore, the critical point can be yielded as

$$p_c = \frac{1}{K}. \tag{A4}$$

As shown in Fig. 7, this result is consistent with the simulation results on the ER random networks, but not with those on the RRGs. We think that this is just a coincidence because the result on the RRGs should theoretically be better than that on the ER random networks. The reason is that the approximate mean-field analysis is established for the dynamical process on annealed networks. However, we can still use this method to draw some useful information [50].

In scale-free networks, the degree distribution is highly skewed and the homogeneous mixing hypothesis is no longer applicable. To resolve the degree variation of the neurons, we calculate the density $\rho_t^k(1)$ of the excited neurons with degree k by assuming the equivalence of all neurons of degree k. The extended mean-field equation can be written as [12,48]

$$\partial_t \rho_t^k(1) = -\rho_t^k(1) + \lambda\rho_t^k(0) + kp(1-\lambda)\rho_t^k(0)\Theta(\rho_t(1)), \tag{A5}$$

where the third term indicates that the newly increased excited neurons is proportional to the probability $\rho_t^k(0)$ that a resting neuron has degree k, the probability $\Theta(\rho_t(1))$ that any given link points to an excited neuron, and the probability p that it is excited by that excited neighbor. The factor k indicates all the possible edges through which the resting neuron can be excited by its neighbors.

By imposing the stationarity condition $\partial_t \rho_t(1) = 0$, we obtain

$$\rho^k(1) = \frac{\lambda + (1-\lambda)pk\Theta(\lambda,p)}{1+(n-1)[\lambda+(1-\lambda)pk\Theta(\lambda,p)]}. \tag{A6}$$

In uncorrelated random networks, the probability that an edge points to a neuron with degree k' is independent of the degree

k of the neuron from which the edge is emanating. We assume that Θ is a function of the total density of excited nodes $\rho(1)$ (so that it is a function of λ and p). Therefore, as in [12], we can obtain

$$\Theta(\lambda,p)=\frac{1}{K}\sum_k kP_k\rho^k(1). \tag{A7}$$

It is easy to calculate $\Theta(\lambda,p)$ by using the above self-consistency equation. Combining Eqs. (A6) and (A7) yields the density $\rho^k(1)$ of the excited neurons with degree k. Then, we can evaluate the total density $\rho(1)$ of the excited neurons by

$$\rho(1)=\sum_k P_k\rho^k(1). \tag{A8}$$

In our study, we construct the uncorrelated random SF network by using the configuration algorithm. The degree distribution can be written as

$$P_k=\frac{1-\gamma}{k_{\max}^{1-\gamma}-m^{1-\gamma}}k^{-\gamma}, \tag{A9}$$

and the average degree is

$$K=\int_m^{k_{\max}}P_k k\,dk=\frac{\gamma-1}{\gamma-2}\frac{m^{2-\gamma}-k_{\max}^{2-\gamma}}{m^{1-\gamma}-k_{\max}^{1-\gamma}}, \tag{A10}$$

where m is the minimum degree (we set $m=2$ in the current study) and $k_{\max}$ is the maximum degree. Then, Eq. (A7) becomes

$$\Theta(\lambda,p)=\frac{1}{K}\int_m^{k_{\max}}kP_k\rho^k(1)dk, \tag{A11}$$

and we can obtain

$$\Theta(\lambda,p)=\frac{1}{n-1}+\frac{\gamma-2}{(n-1)ab_2}\big[b_1+k_{\max}^{1-\gamma}\mathscr{F}(1,1-\gamma,2-\gamma,k_{\max}c)-m^{1-\gamma}\mathscr{F}(1,1-\gamma,2-\gamma,mc)\big], \tag{A12}$$

where $a=(n-1)(\gamma-1)(1-\lambda)p\Theta(\lambda,p)$, $b_1=m^{1-\gamma}-k_{\max}^{1-\gamma}$, $b_2=m^{2-\gamma}-k_{\max}^{2-\gamma}$, $c=\frac{a}{1+(n-1)\lambda}$, and $\mathscr{F}$ is the Gauss hypergeometric function [51]. Obviously, it is quite difficult to resolve the above equation, and we cannot obtain a general formula to describe the dynamics of neural activity.

APPENDIX B: DERIVATION OF EQ. (12)

For the Kinouchi-Copelli neural model on the RRGs, we consider how the classes of $X_{K,0,0}$, $X_{K-1,1,0}$, and $X_{K-1,0,1}$ ($X\in\{R,S,T\}$) change with respect to time. First, Eq. (7) can be simplified as

$$\begin{aligned}R_{K,0,0}(t+1)&=R_{K,0,0}(t)(1-P_R)^K\\&\quad+R_{K-1,0,1}(t)(1-P_R)^{K-1}\\&\quad+T_{K,0,0}(t)(1-P_T)^K\\&\quad+T_{K-1,0,1}(t)(1-P_T)^{K-1},\end{aligned}$$

$$\begin{aligned}R_{K-1,1,0}(t+1)&=R_{K,0,0}(t)\binom{K}{1}P_R(1-P_R)^{K-1}\\&\quad+R_{K-1,0,1}(t)\binom{K-1}{1}P_R(1-P_R)^{K-2}\\&\quad+T_{K,0,0}(t)\binom{K}{1}P_T(1-P_T)^{K-1}\\&\quad+T_{K-1,0,1}(t)\binom{K-1}{1}P_T(1-P_T)^{K-2},\\R_{K-1,0,1}(t+1)&=R_{K-1,1,0}(t)(1-P_R)^{K-1}(1-p)\\&\quad+T_{K-1,1,0}(t)(1-P_T)^{K-1},\end{aligned} \tag{B1}$$

$$\begin{aligned}S_{K,0,0}(t+1)=0,\quad S_{K-1,1,0}(t+1)=0,\\S_{K-1,0,1}(t+1)=R_{K-1,1,0}(t)(1-P_R)^{K-1}p,\end{aligned} \tag{B2}$$

$$\begin{aligned}T_{K,0,0}(t+1)&=S_{K-1,0,1}(t)(1-P_S)^{K-1},\\T_{K-1,1,0}(t+1)&=S_{K-1,0,1}(t)\binom{K-1}{1}P_S(1-P_S)^{K-2},\\T_{K-1,0,1}(t+1)&=0.\end{aligned} \tag{B3}$$

Substituting Eqs. (B2) and (B3) into Eq. (B1) and omitting the subscript t in the stationary state, we obtain

$$\begin{aligned}R_{K,0,0}&=R_{K,0,0}(1-P_R)^K+R_{K-1,0,1}(1-P_R)^{K-1}\\&\quad+pR_{K-1,1,0}(1-P_R)^{K-1}(1-P_S)^{K-1}(1-P_T)^K,\\R_{K-1,1,0}&=KR_{K,0,0}P_R(1-P_R)^{K-1}\\&\quad+(K-1)R_{K-1,0,1}P_R(1-P_R)^{K-2}\\&\quad+KpR_{K-1,1,0}(1-P_R)^{K-1}(1-P_S)^{K-1}P_T\\&\quad\times(1-P_T)^{K-1},\\R_{K-1,0,1}&=(1-p)R_{K-1,1,0}(1-P_R)^{K-1}\\&\quad+(K-1)pR_{K-1,1,0}(1-P_R)^{K-1}P_S(1-P_S)^{K-2}\\&\quad\times(1-P_T)^{K-1}.\end{aligned} \tag{B4}$$

The probabilities of the subscript transformation in these approximations can be obtained by using Eq. (B2), Eq. (B3), and ignoring higher-order terms of P_R,

$$\begin{aligned}P_R&=\frac{(K-1)R_{K-1,1,0}}{KR_{K,0,0}+(K-1)(R_{K-1,1,0}+R_{K-1,0,1})}\\&\approx\frac{(K-1)R_{K-1,1,0}}{KR_{K,0,0}+(K-1)R_{K-1,1,0}},\end{aligned} \tag{B5}$$

$$\begin{aligned}P_S&=\frac{R_{K-1,1,0}\cdot p}{KS_{K,0,0}+(K-1)(S_{K-1,1,0}+S_{K-1,0,1})}\\&=\frac{1}{(K-1)(1-P_R)^{K-1}}\approx\frac{1}{(K-1)},\end{aligned} \tag{B6}$$

$$P_T=0. \tag{B7}$$

Combining these expressions with Eq. (B4), and ignoring higher-order terms of P_R, leads to

$$\begin{aligned}AR_{K,0,0}+BR_{K-1,1,0}=0,\\CR_{K,0,0}+DR_{K-1,1,0}=0,\end{aligned} \tag{B8}$$

where

$$z = \frac{K-2}{K-1}, \quad A = K\left(1 - Kp + p\frac{2K-3}{K-1}z^{K-2}\right),$$
$$B = (K-1)\Big\{(1+p)[1+2(K-1)p] + p\frac{2K-3}{K-1}z^{K-2} - p^2(2K-3)z^{K-2}\Big\},$$
$$C = K[(K-1)p-1],$$
$$D = (K-1)^2(p-p^2-1+p^2z^{K-2}). \tag{B9}$$

APPENDIX C: APPROXIMATE-MASTER-EQUATION APPROACH (AMEA) FOR THE ASYNCHRONOUS UPDATE MODEL

1. Details for the AMEA

Similar to what we have defined in the synchronous updating of the Kinouchi-Copelli neural model, each neuron can be categorized by its state and the number of its neighbors in each state. Let $X_{i,j,l}$ $(X \in \{R,S,T\})$ be the number of X neurons with i resting neighbors, j excited neighbors, and l refractory neighbors. When one neighbor of a neuron is excited, the excited degree increases by 1 and the resting degree decreases by 1, respectively. The neuron in the $X_{i,j,l}(t)$ class will join the $X_{i-1,j+1,l}(t+1)$ class at the next time step. The rate of new excited neurons is $\sum_k^{k_{\max}}\sum_{i+j+l=k}(pj+\lambda)R_{i,j,l}$. The effective degree of the resting neighbors is changed by these new excited neurons at the rate $\sum_k^{k_{\max}}\sum_{i+j+l=k} i(pj+\lambda)R_{i,j,l}$. Then the rate at which the neurons in the $R_{\alpha+1,\beta-1,\gamma}$ class will join the $R_{\alpha,\beta,\gamma}$ class (due to the influence of the excited neighbors) is

$$W(R_{\alpha+1,\beta-1,\gamma} \to R_{\alpha,\beta,\gamma}) = \frac{\sum_k^{k_{\max}}\sum_{i+j+l=k} i(pj+\lambda)R_{i,j,l}}{\sum_k^{k_{\max}}\sum_{i+j+l=k} iR_{i,j,l}}(\alpha+1)R_{\alpha+1,\beta-1,\gamma}. \tag{C1}$$

Following the same argument, we obtain

$$W(R_{\alpha,\beta+1,\gamma-1} \to R_{\alpha,\beta,\gamma}) = (\beta+1)R_{\alpha,\beta+1,\gamma-1}, \tag{C2}$$

$$W(R_{\alpha-1,\beta,\gamma+1} \to R_{\alpha,\beta,\gamma}) = (\gamma+1)R_{\alpha-1,\beta,\gamma+1}, \tag{C3}$$

$$W(R_{\alpha,\beta,\gamma} \to R_{\alpha-1,\beta+1,\gamma}) = \frac{\sum_k^{k_{\max}}\sum_{i+j+l=k} i(pj+\lambda)R_{i,j,l}}{\sum_k^{k_{\max}}\sum_{i+j+l=k} iR_{i,j,l}}\alpha R_{\alpha,\beta,\gamma}, \tag{C4}$$

$$W(R_{\alpha,\beta,\gamma} \to R_{\alpha,\beta-1,\gamma+1}) = \beta R_{\alpha,\beta,\gamma}, \tag{C5}$$

$$W(R_{\alpha,\beta,\gamma} \to R_{\alpha+1,\beta,\gamma-1}) = \gamma R_{\alpha,\beta,\gamma}. \tag{C6}$$

The schematic illustration of the asynchronous update model is summarized in Fig. 8. The change of the $R_{\alpha,\beta,\gamma}$ class with respective to time can be written as

$$\begin{aligned}\dot{R}_{\alpha,\beta,\gamma} &= -W(R_{\alpha,\beta,\gamma} \to S_{\alpha,\beta,\gamma}) + W(T_{\alpha,\beta,\gamma} \to R_{\alpha,\beta,\gamma}) \\ &\quad - W(R_{\alpha,\beta,\gamma} \to R_{\alpha-1,\beta+1,\gamma}) \\ &\quad + W(R_{\alpha+1,\beta-1,\gamma} \to R_{\alpha,\beta,\gamma}) \\ &\quad - W(R_{\alpha,\beta,\gamma} \to R_{\alpha,\beta-1,\gamma+1}) \\ &\quad + W(R_{\alpha,\beta+1,\gamma-1} \to R_{\alpha,\beta,\gamma}) \\ &\quad - W(R_{\alpha,\beta,\gamma} \to R_{\alpha+1,\beta,\gamma-1}) \\ &\quad + W(R_{\alpha-1,\beta,\gamma+1} \to R_{\alpha,\beta,\gamma}) \\ &= -(p\beta+\lambda)R_{\alpha,\beta,\gamma} + T_{\alpha,\beta,\gamma} - G'\alpha R_{\alpha,\beta,\gamma} \\ &\quad + G'(\alpha+1)R_{\alpha+1,\beta-1,\gamma} - \beta R_{\alpha,\beta,\gamma} \\ &\quad + (\beta+1)R_{\alpha,\beta+1,\gamma-1} - \gamma R_{\alpha,\beta,\gamma} \\ &\quad + (\gamma+1)R_{\alpha-1,\beta,\gamma+1},\end{aligned} \tag{C7}$$

where

$$G' = \frac{\sum_k^{k_{\max}}\sum_{i+j+l=k} i(pj+\lambda)R_{i,j,l}}{\sum_k^{k_{\max}}\sum_{i+j+l=k} iR_{i,j,l}}. \tag{C8}$$

We can also derive the equations for $S_{\alpha,\beta,\gamma}$ and $T_{\alpha,\beta,\gamma}$ in the same way, which yields

$$\begin{aligned}\dot{S}_{\alpha,\beta,\gamma} &= -S_{\alpha,\beta,\gamma} + (p\beta+\lambda)R_{\alpha,\beta,\gamma} - H'\alpha S_{\alpha,\beta,\gamma} \\ &\quad + H'(\alpha+1)S_{\alpha+1,\beta-1,\gamma} - \beta S_{\alpha,\beta,\gamma} \\ &\quad + (\beta+1)S_{\alpha,\beta+1,\gamma-1} - \gamma S_{\alpha,\beta,\gamma} + (\gamma+1)S_{\alpha-1,\beta,\gamma+1},\end{aligned} \tag{C9}$$

$$\begin{aligned}\dot{T}_{\alpha,\beta,\gamma} &= -R_{\alpha,\beta,\gamma} + S_{\alpha,\beta,\gamma} - O'\alpha T_{\alpha,\beta,\gamma} \\ &\quad + O'(\alpha+1)T_{\alpha+1,\beta-1,\gamma} - \beta T_{\alpha,\beta,\gamma}\end{aligned}$$

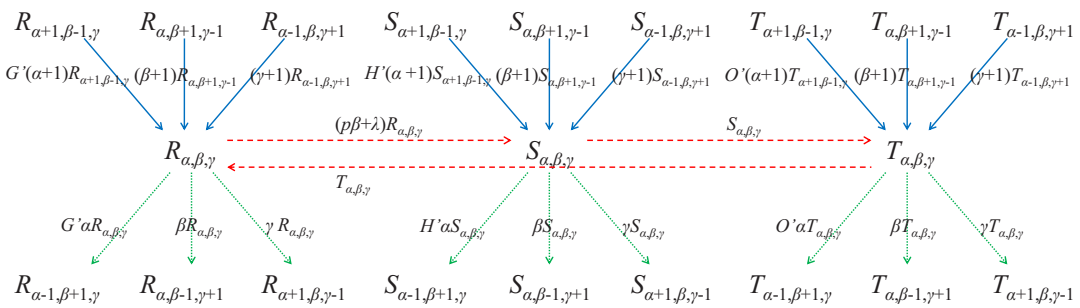

FIG. 8. Schematic illustration of the transitions of the dynamics of the asynchronous update model. There is only one neuron updating its state at each time step. The dashed arrows represent the change of neuronal states, while the solid arrows and the dotted arrows represent the changes induced by the state transformation of the neuron's neighbors. Expressions over the lines are the probabilities of transformations.

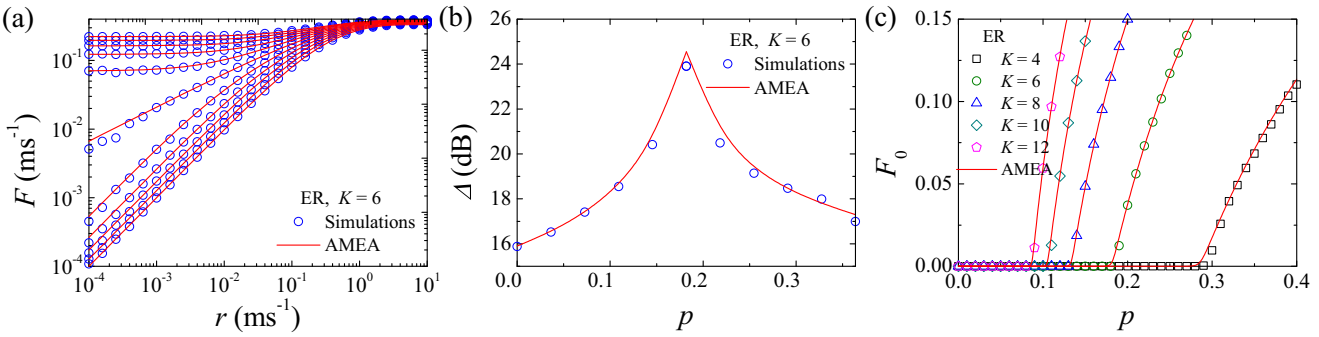

FIG. 9. (a) Response curves F as a function of r of the asynchronous update model on ER random networks with $N = 10^4$, $K = 6$ (from $p = 0$ to 0.363 80 in intervals of 0.036 38). (b) Dynamic range Δ vs the branching probability p on ER random networks. (c) Minimum response F_0 on the ER random networks. Results from stochastic simulations are averaged over 10 independent realizations.

$$+(\beta+1)T_{\alpha,\beta+1,\gamma-1}-\gamma T_{\alpha,\beta,\gamma}$$
$$+(\gamma+1)T_{\alpha-1,\beta,\gamma+1}, \tag{C10}$$

where

$$H'=\frac{\sum_k^{k_{\max}}\sum_{i+j+l=k} j(pj+\lambda)R_{i,j,l}}{\sum_k^{k_{\max}}\sum_{i+j+l=k} iS_{i,j,l}}, \tag{C11}$$

$$O'=\frac{\sum_k^{k_{\max}}\sum_{i+j+l=k} l(pj+\lambda)R_{i,j,l}}{\sum_k^{k_{\max}}\sum_{i+j+l=k} iT_{i,j,l}}. \tag{C12}$$

The dynamics of the asynchronous update model is determined by Eqs. (C7)–(C10). With the initial conditions given by Eq. (8), we are able to obtain the expected results conveniently.

2. The Gillespie Algorithm

We implement the stochastic simulations of the asynchronous update model by using the Gillespie algorithm [52,53] in continuous time. The algorithm is operated in the following way. (i) Choose randomly a faction ρ_0 of neurons as excited seeds at time $t = 0$. (ii) Calculate each neuron's transition rate $a_i(t)$ at time t. The rate for the resting neuron i becoming excited is $a_i(t) = p \times k_{\text{exc}}$, where k_{exc} is the number of the excited neighbors of neuron i, and the rate for each excited neuron going into the refractory period, or each refractory neuron going into the resting state, is 1. Then we can obtain the total transition rate $a(t) = \sum_i a_i(t)$. (iii) Generate a random pair (u,v) with $u,v \in [0,1)$ if $\sum_{i=1}^{j-1}\frac{a_i(t)}{a(t)} < u < \sum_{i=1}^{j}\frac{a_i(t)}{a(t)}$. Then neuron j is chosen to change its state, and time $t' = t + \Delta t$ is an exponentially distributed time step with mean $\frac{1}{a(t)}$, where $\Delta t = \frac{1}{a(t)}\ln(\frac{1}{v})$. (iv) Repeat steps (ii) and (iii) until the system reaches the stationary state.

3. Results

With the same approach used in the synchronous update model, we make a cutoff of the transient process in the asynchronous update model by letting the system evolve 200 ms and then counting the quantities in the next 100 ms. The integrative time step adopted in the AMEA is 10^{-3} ms, and it should be small enough that the size of the $X_{\alpha,\beta,\gamma}$ ($X \in \{R,S,T\}$) classes shown in Eqs. (C7)–(C10) will not be negative. We plot the results of the response curves F and the corresponding dynamic range Δ on ER random networks with $K = 6$, the minimum response F_0 on ER random networks with different K in Fig. 9. It is obvious that these results are in good agreement with those from stochastic simulations.

[1] S. S. Stevens, in *Psychophysics: Introduction to Its Perceptual, Neural and Social Prospects*, edited by G. Stevens (Wiley, New York, 1975).
[2] L. E. Krueger, Behav. Brain Sci. **12**, 251 (1989).
[3] O. Kinouchi and M. Copelli, Nat. Phys. **2**, 348 (2006).
[4] T. L. Ribeiro and M. Copelli, Phys. Rev. E **77**, 051911 (2008).
[5] G. Buzsáki, *Rhythms of the Brain* (Oxford University Press, New York, 2006).
[6] J. G. Nicholls, A. R. Martin, P. A. Fuchs, D. A. Brown, M. E. Diamond, and D. Weisblat, *From Neuron to Brain*, 5th ed. (Sinauer Associates, Sunderland, USA, 2012).
[7] J.-P. Eckmann, O. Feinerman, L. Gruendlinger, E. Moses, J. Soriano, and T. Tlusty, Phys. Rep. **449**, 54 (2007).
[8] T. Kosaka and K. Kosaka, Neurosci. Res. **45**, 189 (2003).
[9] C. Zhang and D. Restrepo, J. Comp. Neurol. **459**, 426 (2003).
[10] M. R. Deans, B. Volgyi, D. A. Goodenough, S. A. Bloomfield, and D. L. Paul, Neuron **36**, 703 (2002).
[11] M. Copelli and P. R. A. Campos, Eur. Phys. J. B **56**, 273 (2007).
[12] A.-C. Wu, X.-J. Xu, and Y.-H. Wang, Phys. Rev. E **75**, 032901 (2007).
[13] D. B. Larremore, W. L. Shew, and J. G. Restrepo, Phys. Rev. Lett. **106**, 058101 (2011).
[14] D. B. Larremore, W. L. Shew, E. Ott, and J. G. Restrepo, Chaos **21**, 025117 (2011).
[15] S. Pei, S. Tang, S. Yan, S. Jiang, X. Zhang, and Z. Zheng, Phys. Rev. E **86**, 021909 (2012).
[16] W. L. Shew, H. Yang, T. Petermann, R. Roy, and D. Plenz, J. Neurosci. **29**, 15595 (2009).
[17] M. Copelli, *Criticality in Neural Systems* (Wiley-VCH Verlag, Weinheim, Germany, 2014), pp. 347–364.

[18] L. L. Gollo, C. Mirasso, and V. M. Eguíluz, Phys. Rev. E **85**, 040902 (2012).
[19] V. R. V. Assis and M. Copelli, Phys. Rev. E **77**, 011923 (2008).
[20] L. L. Gollo, O. Kinouchi, and M. Copelli, Phys. Rev. E **85**, 011911 (2012).
[21] C. Haldeman and J. M. Beggs, Phys. Rev. Lett. **94**, 058101 (2005).
[22] J. Lindquist, J. Ma, P. van den Driessche, and F. Willeboordse, J. Math. Biol. **62**, 143 (2011).
[23] C.-R. Cai, Z.-X. Wu, and J.-Y. Guan, Phys. Rev. E **90**, 052803 (2014).
[24] J. P. Gleeson, Phys. Rev. Lett. **107**, 068701 (2011).
[25] J. P. Gleeson, Phys. Rev. X **3**, 021004 (2013).
[26] P. Erdös and A. Rényi, Publ. Math. Debrecen **6**, 290 (1959).
[27] B. Bollobás, *Random Graphs*, 2nd ed. (Cambridge University Press, Cambridge, 2001).
[28] M. E. J. Newman, *Networks: An Introduction* (Oxford University Press, New York, 2010).
[29] M. Catanzaro, M. Boguñá, and R. Pastor-Satorras, Phys. Rev. E **71**, 027103 (2005).
[30] M. Copelli, A. C. Roque, R. F. Oliveira, and O. Kinouchi, Phys. Rev. E **65**, 060901 (2002).
[31] M. Copelli and O. Kinouchi, Physica A **349**, 431 (2005).
[32] S. Haykin, *Neural Networks and Learning Machines*, 3rd ed. (Prentice Hall, New York, 2008).
[33] S. N. Dorogovtsev, A. V. Goltsev, and J. F. F. Mendes, Rev. Mod. Phys. **80**, 1275 (2008).
[34] R. Legenstein and W. Maass, Neural Netw. **20**, 323 (2007).
[35] J. M. Beggs and D. Plenz, J. Neurosci. **23**, 11167 (2003).
[36] R. Der, F. Hesse, and G. Martius, Adapt. Behav. **14**, 105 (2006).
[37] D. R. Chialvo, Nat. Phys. **2**, 301 (2006).
[38] D. Plenz and T. C. Thiagarajan, Trends Neurosci. **30**, 101 (2007).
[39] A. Levina, J. M. Herrmann, and T. Geisel, Nat. Phys. **3**, 857 (2007).
[40] A. Levina, J. M. Herrmann, and T. Geisel, Phys. Rev. Lett. **102**, 118110 (2009).
[41] A. Levina, J. M. Herrmann, and T. Geisel, *Criticality in Neural Systems* (Wiley-VCH Verlag, Weinheim, Germany, 2014), pp. 417–436.
[42] K.-E. Lee, M. A. Lopes, J. F. F. Mendes, and A. V. Goltsev, Phys. Rev. E **89**, 012701 (2014).
[43] M. A. Lopes, K.-E. Lee, A. V. Goltsev, and J. F. F. Mendes, Phys. Rev. E **90**, 052709 (2014).
[44] A. Clauset, C. R. Shalizi, and M. E. J. Newman, SIAM Rev. **51**, 661 (2009).
[45] Y. Adini, D. Sagi, and M. Tsodyks, Proc. Natl. Acad. Sci. USA **94**, 10426 (1997).
[46] F. Borges, E. Lameu, A. Batista, K. Iarosz, M. Baptista, and R. Viana, Physica A **430**, 236 (2015).
[47] R. Viana, F. Borges, K. Iarosz, A. Batista, S. Lopes, and I. Caldas, Commun. Nonlin. Sci. Numer. Simul. **19**, 164 (2014).
[48] J. Marro and R. Dickman, *Nonequilibrium Phase Transitions in Lattice Models* (Cambridge University Press, Cambridge, 1999).
[49] L. S. Furtado and M. Copelli, Phys. Rev. E **73**, 011907 (2006).
[50] A. Barrat, M. Barthlemy, and A. Vespignani, *Dynamical Processes on Complex Networks* (Cambridge University Press, Cambridge, 2008).
[51] M. Abramowitz and I. A. Stegun, *Handbook of Mathematical Functions* (Dover, New York, 1972).
[52] D. T. Gillespie, J. Comput. Phys. **22**, 403 (1976).
[53] D. T. Gillespie, J. Phys. Chem. **81**, 2340 (1977).